

6. CONCLUSION

A new type of planar transmission line, modified from the traditional Goubaud line, has been proposed. Some different configurations have been demonstrated and the dimensions of this new type of transmission line have been provided. The numerical results, suitable for practical applications, were obtained by using the FEM to obtain the solutions. Comparisons with metallic rectangular waveguide have been given. The analysis shows that this new type of transmission line has advantages such as simplicity, ease of fabrication, and low loss, in comparison with other types of transmission lines at terahertz frequencies.

ACKNOWLEDGMENT

The authors are grateful to Natural Science and Engineering Research Council of Canada (NSERC) for financial support.

REFERENCES

1. A.G. Engel, Jr. and P.B. Katehi, Low-loss monolithic transmission lines for submillimeter and terahertz frequency applications, *IEEE Trans Microwave Theory Tech MTT-39* (1994), 1847–1854.
2. N.-H. Huynh and W. Heinrich, FDTD analysis of submillimeter-wave CPW with finite-width ground metallization, *IEEE Microwave Guided Wave Lett 7* (1997), 414–416.
3. A. Reichelt and I. Wolff, New coplanar-like transmission lines for application in monolithic integrated millimeter-wave and submillimeter-wave circuits, *IEEE MTT-S Dig* (1998), Baltimore, MD, 99–102.
4. T. Suzuki, N. Kakizaki, and Y. Watanabe, Study of in-situ gas sensor based on millimeter/submillimeter wave spectroscopy, *Proc Int Symp Antennas Propagat (ISAP)*, 2000, Salt Lake City, UT, p. 971.
5. K. Maeda, Y. Iida, and T. Manabe, Protection of space borne and terrestrial passive sensors to observe trace gasses from 200 to 700 GHz, *IEEE Int Geosci and Remote Sensing Symp*, 2000, p. 2467.
6. M. Coulombe, J. Waldman, R. Giles, A. Gatesman, T. Goyette, and W. Nixon, Submillimeter-wave polarimetric compact ranges for scale-model radar measurements, *IEEE MTT-S Dig* (2002) Seattle, WA, 1583–1586.
7. K. Alonso and M.J. Hagmann, Simulations of tapered Goubaud line for coupling of microwave signals generated by resonant laser-assisted field emission, *J Vacuum Sci Technol B* 18 (2000), 1009–1013.
8. K. Alonso and M.J. Hagmann, Comparison of three different methods for coupling of microwave signals generated by resonant laser-assisted field emission, *J Vacuum Sci Technol B* 19 (2001), 68–71.
9. G. Goubaud, Surface waves and their application to transmission line, *J Appl Phys* 21 (1950), 1119–1128.
10. G. Goubaud, Single-conductor surface-wave transmission lines, *Proc IRE* 39 (1951), 619–624.
11. M.J. King and J.C. Wiltse, Surface-wave propagation on coated or uncoated metal wires at millimeter wavelengths, *IRE Trans Antennas Propagat AP-10* (1962), 246–254.
12. J.A. Stratton, *Electromagnetic theory*, McGraw-Hill, New York, 1941, pp. 527–531.
13. Sakina and J. Chiba, Resonant mode of surface wave in Goubaud line, *IEICE Trans Electron E-76-C* (1993), 657–660.
14. J.G. Fikioris and J.A. Roumeliotis, Cutoff wave-numbers of Goubaud lines, *IEEE Trans Microwave Theory Tech MTT-27* (1979), 570–573.
15. Y. Seo and W. Jhe, High-speed near-field scanning optical microscopy with a quartz crystal resonator, *Rev Scientific Instrum* 73 (2002), 2057–2059.

© 2004 Wiley Periodicals, Inc.

AN ACTIVE RECEIVING ANTENNA FOR SHORT-RANGE WIRELESS AUTOMOTIVE COMMUNICATION

Basim Al-Khateeb,¹ Victor Rabinovich,² and Barbara Oakley³

¹ Daimler Chrysler Corporation

800 Chrysler Drive
Auburn Hills, MI

² Tenatronics Ltd.

776 Davis Drive
Newmarket, Ontario, Canada

³ Department of Electrical and Systems Engineering
Oakland University
Rochester, MI

Received 22 April 2004

ABSTRACT: This paper describes an easily manufactured, reduced-size, active receiving antenna for automotive applications, which increases short-range wireless detection in the 315-MHz band. This compact antenna has an advantage over currently available antennas because it can be hidden in a vehicle's interior. The active antenna consists of a low-noise amplifier coupled to a low-profile planar meander-line pattern printed on the dielectric substrate. Experimental verification of the antenna performance and a theoretical calculation for the maximum range of the active antenna are presented. © 2004 Wiley Periodicals, Inc. *Microwave Opt Technol Lett* 43: 293–297, 2004; Published online in Wiley InterScience (www.interscience.wiley.com). DOI 10.1002/mop.20449

Key words: active receiving antenna; low-noise amplifier; printed meander-line antenna; short-range wireless communication

1. INTRODUCTION

Wireless devices such as remote-control engine start systems, keyless entry systems, and automatic tolling systems are now considered “classical” devices for short-range vehicle wireless communication [1, 2]. Such control and security devices commonly use the 315-MHz frequency band in the United States and Canada. The receiving antenna is vital to the performance of such systems.

Dipole antennas designed for use in the 315-MHz frequency band are large and inconvenient for interior vehicle applications. An alternative antenna type for vehicular use would appear to be a miniature printed circuit-board antenna. However, such a small electrically sized passive antenna has one significant disadvantage: low radiating efficiency, with concomitant low gain and short communication range [3, 4]. Problems with passive antennas have led investigators towards active antennas, which in recent years have been designed for use in the 800-MHz and higher range for Bluetooth, GPS, satellite digital radio, and mobile-phone technologies [5–7]. Only a few researchers have proposed active printed dipole antennas in the 300–500-MHz frequency band [8, 9]. However, these antennas are more than 200 cm in size and are therefore too large for in-vehicle applications. Despite the need for such devices, to our knowledge, miniature printed circuit-board active antennas in the 300–500-MHz frequency range have not been previously investigated. This paper describes a small electrically sized active printed meander-line antenna for short-range automotive wireless communication in the 315-MHz frequency band. The maximum operating range, as a function of the active antenna parameters (amplifier gain, amplifier noise figure, and antenna gain), and the sensitivity of the receiver, is estimated over a wide range of short-wave communication frequencies.

Antenna-pattern performances are very specific to the location of the antenna on the vehicle [10–12]. Reflections and shadowing

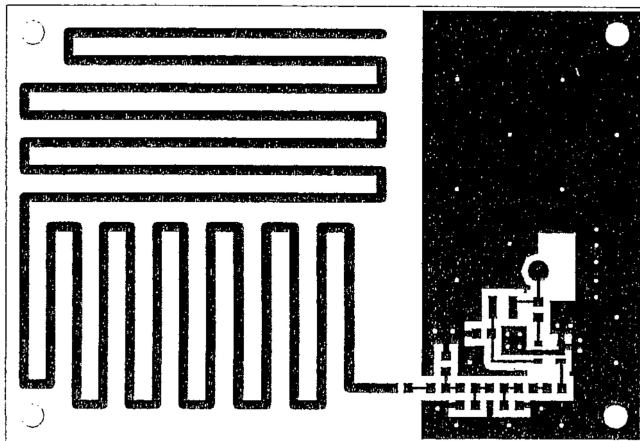


Figure 1 Geometry of the proposed printed meander-line antenna

effects can make significant changes in antenna patterns. Unfortunately, only experimentally determined electromagnetic-field strengths around the vehicle with the antenna in the appropriate mounting position can reveal the antenna's true performance; antenna simulation results calculated using an ideal ground plane provide misleading results. Therefore, the experimental results for spatial-field strengths are also included in this paper.

2. ACTIVE ANTENNA SYSTEM DESIGN

The active antenna system includes both passive and active components with an input matching circuit, transistor, and output matching circuit. Figure 1 shows the geometry of the proposed meander-line antenna.

2.1. Passive Antenna Design

The meander-line component of the antenna has compact dimensions of $50 \times 50 \text{ mm}^2$, and is printed on the front of an FR4 substrate (thickness 1.6 mm and relative permittivity 4.4). The antenna ground plane is printed on the bottom side of the substrate as well as partly on the top side. The bottom ground plane is used at the same time as the ground plane of the amplifier connected to the meander line.

It is well known [13, 14] that a folded wire length in a monopole antenna increases the radiation resistance and consequently the input impedance. With this in mind, the meander-line design was optimized using electromagnetic software IE3D [15] to provide 50Ω impedance and omnidirectional directivity. The simulation results reveal the total radiating antenna efficiency η is 0.15. Figure 2 reveals the measured input impedance and VSWR of the passive antenna component. To make accurate measurements of the antenna impedance, a $\lambda/4$ metal sleeve (balun) was used to eliminate stray current, along with its undesired radiation, from the coaxial cable.

2.2. Active Antenna Design

The amplifier for the antenna was designed using computer software from Eagleware Corporation [16]. Overall amplifier properties were optimized to obtain noise impedance matching between the antenna and transistor stage, and power impedance matching between the amplifier and the 50Ω load. The amplifier consists of a single-stage NE 662 transistor from California Eastern Laboratories coupled to a passive input circuit that provides a low noise figure, and an output matching circuit that provides maximum amplifier gain.

The experimentally measured amplifier gain in the 315-MHz band as a function of frequency is shown in Figure 3. The noise figure of the amplifier is about 2 dB.

3. ANTENNA PATTERN MEASUREMENTS

The measurement site uses an outdoor automobile turntable (Tektronics Ltd.), which can either rotate the antenna under test alone (without a vehicle) or rotate the automobile along with the antenna. The turntable is placed on a hill to block outside reflections from the surrounding environment. The antenna range instrumentation is controlled by a computer that drives the turntable rotation, controls a spectrum analyzer, and transfers measured data to the hard drive and printer. A data point was taken on the 0° elevation amplitude pattern every 2° as the turntable was rotated through a full 360° azimuth. All field-strength measurements are implemented for the designed antenna installed in a 2003 Yukon vehicle (GM).

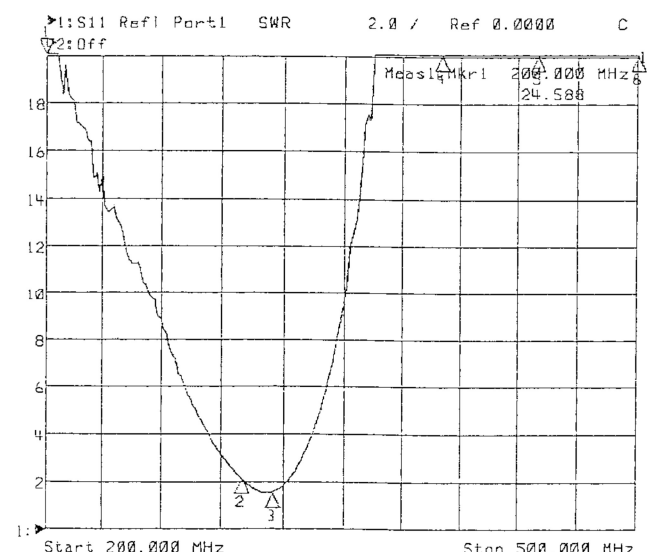
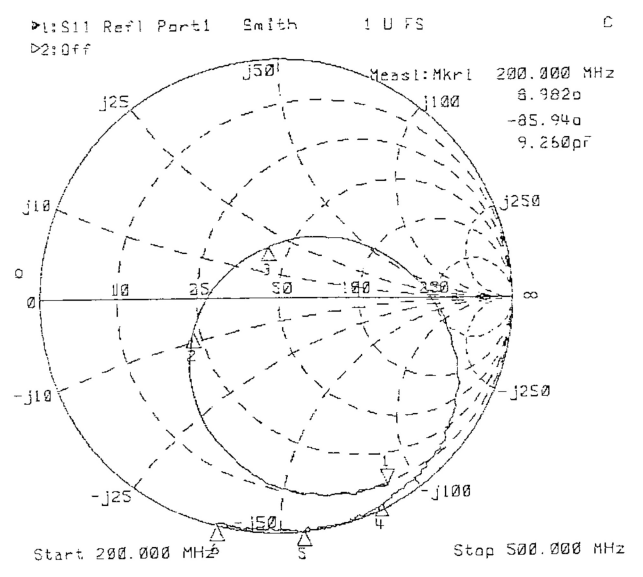


Figure 2 Smith chart and VSWR of the passive antenna part

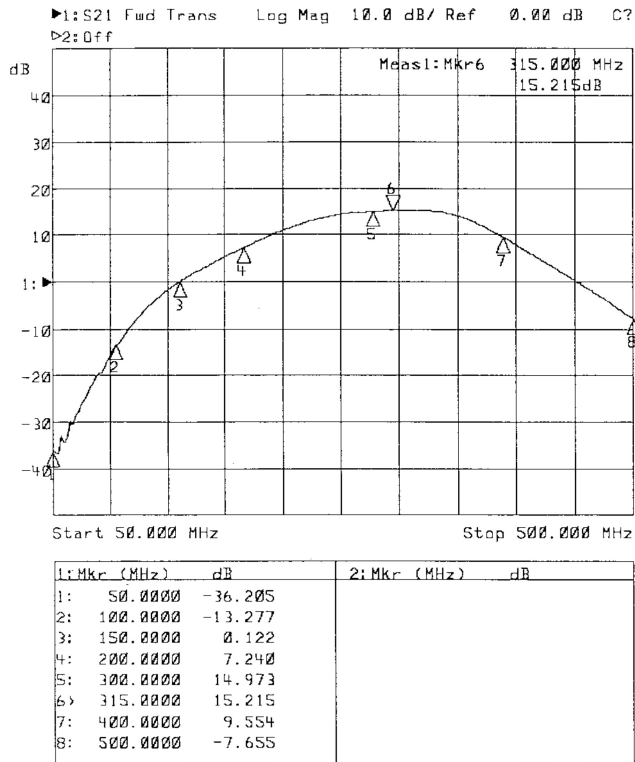


Figure 3 Amplifier gain

For a detailed investigation of the design performance, the antenna prototype was fabricated and measured in two different versions: a passive version without the amplifier and an active version with the amplifier. Since the active antenna has a small size of less than 1/10 of the wavelength, it cannot be considered as purely symmetrical or purely antisymmetrical due to the limited-size ground plane. Classical antenna measurement techniques are consequently no longer adequate due to the current flow on the cable connecting the antenna to the receiver. On the other hand, it is difficult to obtain accurate measurement results of the antenna gain and directionality without the cable and mounting structure. Under such conditions, the only way to obtain a valid gain measurement is to test the antenna, connected through the cable to the receiver, while it is mounted in place on the vehicle. Therefore, all antenna-performance measurements were made when the receiving antenna (either the active antenna or its passive subcomponent) was mounted in this fashion. A transmitting Yagi antenna with horizontal polarization was located the far zone of the antenna receiving system in the vehicle in order to provide signal power for the antenna pattern measurement.

4. ANTENNA PATTERN DATA ANALYSIS

The active antenna system is perhaps best understood by first analyzing the performance of the passive meander-line component of the antenna, then comparing the results with the performance of the meander line coupled to the active antenna. Figure 4 shows the radiation pattern for the meander line alone, without the active antenna, when mounted directly under the front dashboard of the vehicle (the front of the vehicle is located at 320°). The gain value G_a averaged over 360° azimuth is -7.4 dBi, with a standard deviation σ of 4.4 dB. The radiation pattern of a half-wave dipole antenna located at the same place is shown in Figure 5 for comparison. The dipole gain value calculated from the chart data shown in Figure 5 is -2.8 dBi, with a σ of 5.1 dB. The theoretical

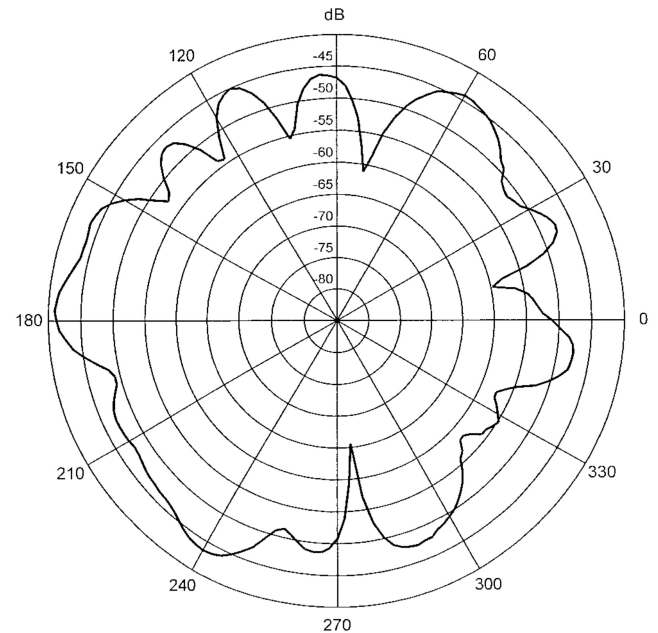


Figure 4 Radiation pattern of the passive meander-line antenna with $G_a = -7.4$ dBi and $\sigma = 4.4$ dB

gain value of the dipole antenna is 2.15 dBi, and the gain value calculated by our antenna from the radiation-efficiency estimation is -8.2 dBi. As can be seen from these results, the vehicle body attenuates the dipole antenna gain, but has minimal effect on the gain value of the meander-line antenna. The difference between the gain values G_a and G_{dipole} measured in the vehicle is 4.6 dBi. Figures 6 and 7 show the radiation-pattern curves for the passive meander-line antenna located on the right-front and rear-roof support pillars of the vehicle. In contrast to the various passive antenna results, Figure 8 reveals the radiation pattern of the active antenna from measurements taken when it was located under the

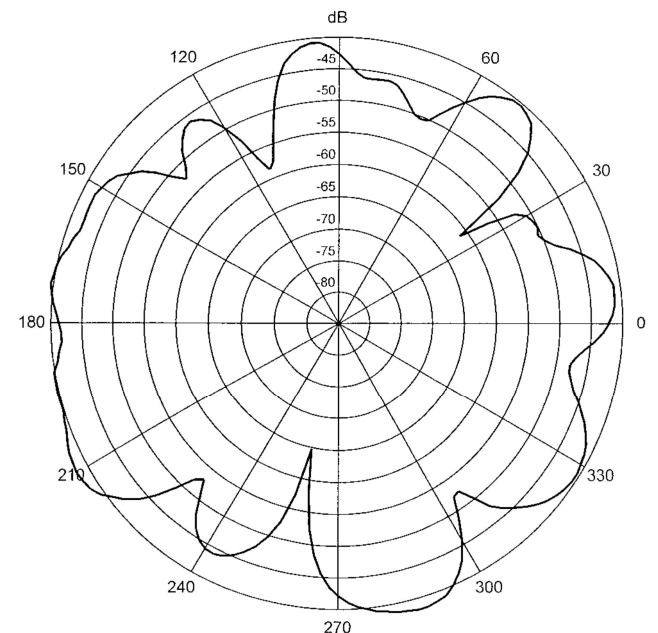


Figure 5 Radiation pattern of the half-wave dipole with $G_a = -2.8$ dBi and $\sigma = 5.1$ dB

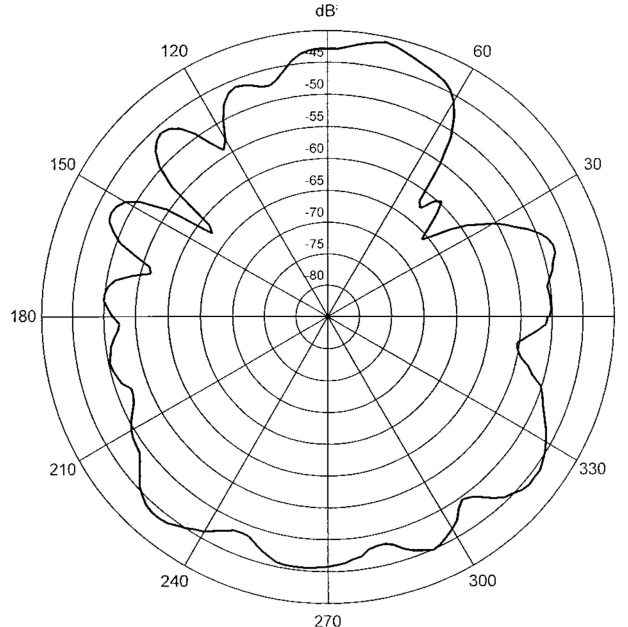


Figure 6 Radiation pattern of the antenna located on the right-front support pillar with $G_a = -7.1$ dBi and $\sigma = 4.9$ dB

front dash of the vehicle. A comparison of the overall active-gain value $G_\Sigma = G_a G_{amp}$ and passive antenna gain G_a shows that the amplifier gain of the active antenna is about 15.4 dB. Neatly affirming these results, this value is approximately the same as the gain of the amplifier alone, as measured in the laboratory.

5. MAXIMUM DETECTION RANGE FOR THE ACTIVE ANTENNA SYSTEM

According to the Friis transmission equation and the pass/loss measurement-based propagation model [17], the signal power at an antenna receiver output is equal to

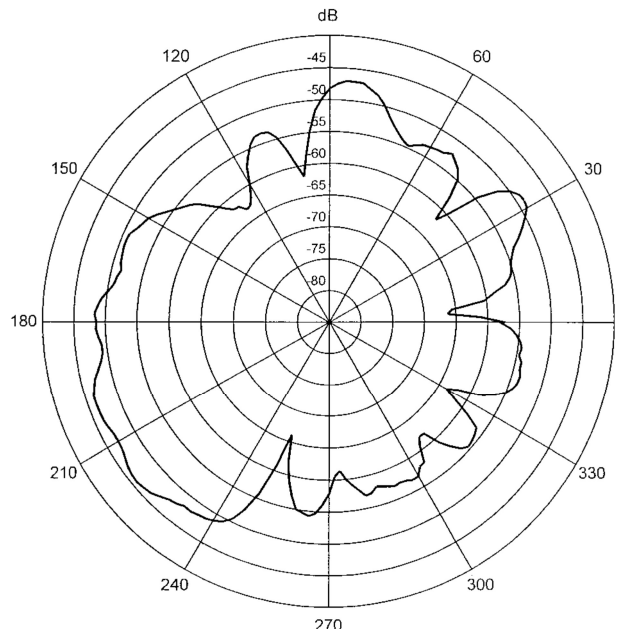


Figure 7 Radiation pattern of the antenna located on the rear-roof support pillar with $G_a = -11.6$ dBi and $\sigma = 4.9$ dB

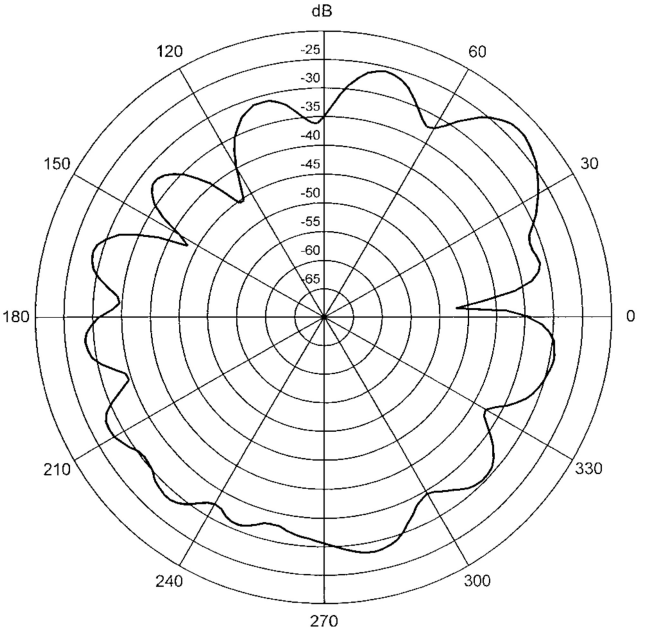


Figure 8 Radiation pattern of the active antenna with $G_\Sigma = 9$ dBi and $\sigma = 4.1$ dB

$$P_r = \frac{P_t G_t G_a G_{amp} G_{rec} \lambda^2}{(4\pi)^2 \cdot D^n}, \quad (1)$$

where λ is the wavelength, P_t is the transmitting power, G_t is the transmitter antenna gain, G_{rec} is the receiver gain, $ERP = P_t \cdot G_t$ is the effective radiated power, D is the distance between the transmitting and receiving antennas, and n is a real constant value that is a function of the wireless communication environment [18].

For free-space propagation, $n = 2$. Extensive measurements have shown that in flat terrain, n is between 2.5 and 4 with an accuracy of ± 6 dB.

Noise power at the receiver output [19] can be estimated as

$$N = kT_0 B G_{amp} G_{rec} \left(\frac{T_a}{T_0} - 1 + \eta - \eta \frac{T_a}{T_0} + F_\Sigma \right), \quad (2)$$

where $F_\Sigma = F_{amp} + (F_{rec} - 1)/G_{amp}$ is the wireless system noise figure, F_{amp} is the amplifier noise figure, F_{rec} is the receiver noise figure, B is the receiver frequency bandwidth, T_a is the antenna noise temperature, $T_0 = 290$ K, and $k = 1.38 \cdot 10^{-23}$ J/K is the Boltzman's constant.

It is known [20] that for the UHF band, $T_a = T_0 = 290$ K. In this case, Eq. (2) can be simplified to:

$$N = kT_0 B G_{amp} G_{rec} F_\Sigma.$$

Using Eq. (1) and the noise-signal value $N = kT_0 B G_{amp} G_{rec} F_\Sigma$, the signal-to-noise ratio at the receiver output can be defined as

$$SNR = \frac{ERP \lambda^2}{(4\pi)^2 D^n k T_0 B F_\Sigma}. \quad (3)$$

According to Eq. (3), the maximum range of the wireless communication system is given by

$$D_{max} = \sqrt[n]{\frac{ERPG_a \lambda^2}{(4\pi)^2 SNR_{min} k T_0 BF_{\Sigma}}}, \quad (4)$$

where SNR_{min} is the minimum signal-to-noise ratio required to detect a signal with the certain probability of the signal detection, and a receiver sensitivity $S = SNR_{min} k T_0 BF_{\Sigma}$. Using Eq. (4), the improvement factor Q in the ratio between the maximum operating distance when using the passive antenna (as opposed to the active antenna) can be estimated. Assuming that SNR_{min} is the same value for the passive and active antenna systems, we can obtain

$$Q_1 = \frac{D_{max}(active)}{D_{max}(passive)} = \sqrt[n]{\frac{F_{rec}}{(F_{amp} + (F_{rec} - 1)/G_{amp})}}. \quad (5)$$

When using a dipole antenna instead of a passive printed antenna, Eq. (5) becomes

$$Q_2 = \frac{D_{max}(active)}{D_{max}(dipole)} = \sqrt[n]{\frac{G_a}{G_{dipole}} \frac{F_{rec}}{(F_{amp} + (F_{rec} - 1)/G_{amp})}}. \quad (6)$$

To illustrate typical results, the following assumptions were made and applied to Eq. (6): receiver sensitivity S is -102 dBm; effective radiated power ERP is -20 dBm; passive antenna gain G_a is -7.4 dBi; G_{amp} is 15 dB; the amplifier noise figure is 2 dB; and the receiver bandwidth is 300 kHz. For the sake of simplicity, the required SNR_{min} ratio (Manchester data) is assumed to be 5 dB. In this case, the receiver noise figure F_{rec} becomes 12.2 dB, while F_{Σ} becomes 3.2 dB. For these data, according to Eqs. (4)–(6), and assuming that for an urban area $n = 2.5$, the maximum range is about 290 m, with improvement factors $Q_1 = 2.3$ and $Q_2 = 1.5$.

The value for n of 2.5 is a approximation for an urban area. Different ranges—sometimes dramatically different—can be observed when making comparisons between areas such as free space, open fields, and high- or low-density parking lots. This is a function of the different reflections from cars, trees, buildings, pavement, soil, and grass. In “real life” then, the detection range is a statistical value, so that Eqs. (4)–(6) represent only average estimates.

The receiver-sensitivity value chosen for the above calculations, -102 dBm, is a real parameter provided by a receiver manufacturer. But the sensitivity of the receiver is a critical detection parameter, which can be seen by exploring the difference in range resulting from minor differences in receiver sensitivities. A receiver from the hypothetical supplier “Mediocre Receivers, Inc.” with sensitivity of -105 dBm, will provide for a maximum range of 310 m, with $Q_1 = 1.8$ and $Q_2 = 1.2$. On the other hand, the receiver from “Fantastic Receivers, Inc.” with sensitivity of -110 dBm, can provide a maximum range of 322 m, with $Q_1 = 1.21$ and $Q_2 = 0.787$. In the latter case, there would be a small increase in range for an active compared with a passive planar antenna, but a decrease in range for the active planar antenna compared to a dipole. This latter case would seem to make the active antenna undesirable, however, the advantages inherent in the active antenna’s ability to be hidden would still conspire to make the antenna an attractive alternative.

6. CONCLUSION

We have demonstrated that a small, flat, meander-line-type active antenna can be used for increased short-range mobile applications. The antenna is designed to be hidden as an interior antenna in the vehicle, and has an extended communication range of over 200 m.

The in-vehicle antenna’s radiation patterns were measured using an automobile turntable. The effects on the radiation pattern of different antenna locations on the vehicle were also investigated. A simple expression was derived that can be used to estimate the improvement in the maximum operating range when using an active-antenna system.

REFERENCES

1. A. Bensky, Short-range wireless communications, Short-range wireless communications, LLH Technology Publishing, 2000.
2. F.L. Dacus, Design of short-range radio systems, Microwaves and RF 40 (2001), 73–80.
3. H.A. Wheeler, Small antennas, IEEE Trans Antennas Propagat AP-23 (1975), 462–469.
4. R.F. Harrington, Effect of antenna size on gain, bandwidth, and efficiency, J Res Nat Stand 64D (1960), 1–12.
5. T.D. Ormiston and P. Gardner, Compact receiving antenna, Electron Lett 34 (1998), 1367–1368.
6. W. Duerr and W. Menzel, A low-noise active receiving antenna using a SiGe HBT, IEEE Microwave Guided Wave Lett 7 (1997), 63–65.
7. V. Rabinovich, L-band active receiving antenna for automotive applications, Microwave Opt Technol Lett 39 (2003), 319–323.
8. M. Taguchi and T. Fujimoto, Actual gain of CPW-fed active integrated antennas for television receiver, IECE Trans Commun E81-B 7 (1998), 1542–1547.
9. M. Taguchi, T. Fujimoto, and K. Tanaka, CPW fed active dipole antenna for television receivers, Electron Lett 30 (1994), 1815–1816.
10. C. Hill and T. Kneisel, Portable radio antenna performance in the 150, 450, 800, and 900 MHz bands outside and in-vehicle, IEEE Trans Vehic Technol 40 (1991), 750–756.
11. M. Daginnus, R. Kronberger, A. Stephan, J. Hopf, and H. Lindenmeier, SDARS antennas: Environmental influences, measurement, vehicle application investigations and field experiences, SAE 2002 World Congress, Society of Automotive Engineers, Detroit, MI, 2002, 2002-01-0120.
12. K. Fujimoto and J.R. James, Mobile antenna systems handbook, Artech House, Boston, 1994, pp. 336–337.
13. S.R. Best, A comparison of the performance properties of the Hilbert curve fractal and meander line monopole antennas, Microwave Opt Technol Lett 35 (2002), 258–262.
14. T.J. Warnagiris and T.J. Minardo, Performance of a meandered line as an electrically small transmitting antenna, IEEE Trans Antennas Propagat AP-46 (1998), 1797–1801.
15. IE3D electromagnetic simulation and optimization software, Zeland Software Inc., www.zeland.com.
16. RF and microwave design software, Eagleware Corporation, www.eagleware.com.
17. T.S. Rappaport, Wireless communications, Prentice Hall, 2002, pp. 138–139.
18. K. Allsebrook and J.D. Parson, Mobile radio propagation in British cities at frequencies in the VHF and UHF bands, IEEE Trans Vehic Technol VT-27 (1978), 313–322.
19. J.D. Kraus and R.J. Marhefka, Antennas, McGraw-Hill, New York, 2002, pp. 409–414.
20. J. Salter, Specifying UHF active antennas and calculating system performance, R&D British Broadcasting Corporation, white paper 066, 2003.

© 2004 Wiley Periodicals, Inc.